ISBN: 978-3-95450-224-0 ISSN: 2673-7035 doi:10.18429/JACoW-FLS2023-TH4A2

A COMPACT INVERSE COMPTON SCATTERING SOURCE BASED ON X-BAND TECHNOLOGY AND CAVITY-ENHANCED HIGH AVERAGE POWER ULTRAFAST LASERS

A. Latina*, V. Muşat, R. Corsini, L. A. Dyks, E. Granados, A. Grudiev, S. Stapnes, P. Wang, W. Wuensch, CERN, Geneva, Switzerland
E. Cormier, G. Santarelli, LP2N, Talence, France

Abstract

A high-pulse-current photoinjector followed by a short high-gradient X-band linac and a Fabry-Pérot enhancement cavity are considered as a driver for a compact Inverse Compton Scattering (ICS) source. Using a high-power ultra-short pulse laser operating in burst mode in a Fabry-Pérot enhancement cavity, we show that outcoming photons with a total flux over 1×10^{13} ph/s and energies in the MeV range are achievable. The resulting high-intensity and high-energy photons allow various applications, including cancer therapy, tomography, and nuclear material detection. A preliminary conceptual design of such a compact ICS source and simulations of the expected performance are presented.

INTRODUCTION

In recent years, research and development of normal-conductive X-band accelerator technologies have seen tremendous progress in the context of the next generation of electron-positron linear colliders, where very high gradients are required to achieve the multi-TeV beam energy target for particle physics. The CLIC Study at CERN is the most notable example, where multi-bunch beams and accelerating gradients three to five times greater than those in currently operating linacs have been demonstrated in prototype accelerator structures [1].

During the last years, alongside X-band developments, laser technology has also undergone significant advancements, with high-power lasers becoming more readily available on the market. At the same time, to generate high-intensity photons, Fabry-Pérot enhancement cavities (FPCs) are becoming widely adopted in inverse Compton scattering sources, as reported in [2, 3].

There has been recent consideration for operating FPCs in pulsed (or burst) mode. FPCs operated in burst mode can achieve effective gains 2 to 3 orders of magnitude larger than in continuous mode, which is the commonly used operation mode in storage-ring-based sources. The operation of FPCs in burst mode is particularly well-suited for inverse Compton scattering sources based on X-band linacs as they have a lower repetition rate than storage rings or energy-recovery linacs [4] and allow for multi-bunch acceleration.

This paper presents the conceptual design of an ICS source based on X-band acceleration and external optical cavity enhancement in an optimised FPC operated in burst mode. By accelerating electrons to 240 MeV energy in less than 10 m, our proposed ICS source could generate gamma photons with energies up to 2 MeV and unprecedented flux and brilliance values. High-quality gamma rays in the MeV energy range can have a wide range of applications in various fields, including material science [5], medicine [6], nuclear physics research [7], homeland security by nuclear resonance fluorescence inspection [8, 9], and nondestructive testing of industrial materials [10]. We named this apparatus HPCI-ICS, which stands for "High Pulse Current Injector driven Inverse Compton Scattering" source.

FACILITY DESCRIPTION

The High-Pulse-Current Injector consists of an S-band photoinjector operating at 3 GHz followed by a high-gradient X-band linac at 12 GHz and a short final focus preparing the beam for the interaction. The main parameters of the facility have been optimised along three axes: (1) ensure high RF power efficiency, (2) maintain beam stability in the linac by reducing the disruptive effects of wakefields, and (3) maximise the photon flux at the IP.

The result is a 12 m long setup that accelerates trains of 1000 electron bunches, each with 100 pC bunch charge, up to 240 MeV with a repetition rate of 100 Hz. These bunches are then collided with a laser beam stored in a burst-mode FPC. Table 1 summarises the main parameters of the facility. A short description of each subsystem is provided in the following sections.

Injector

The S-band photoinjector is similar to that of the CLEAR test facility at CERN [11]. The electrons are released from a photocathode due to the photoelectric effect induced by a UV laser. The single-bunch charge extracted from the cathode is 100 pC. A Cs_2Te cathode was selected due to the small spot size and the limited power required on the laser, thanks to the high quantum efficiency of this semiconductor. The photocathode is located at the centre of the half-cell of a 2.5-cell standing-wave electron gun with a cathode peak gradient of 90 MV/m, immersed in a solenoid field. The total length of the injector is 1.3 m, which accounts for diagnostics and trajectory correctors. Table 2 summarises the main parameters of the injector.

Linac

The X-band linac starts 1.3 m downstream of the cathode and operates at a repetition rate of 100 Hz with an average gradient of 35 MV/m. The linac consists of three X-band

* andrea.latina@cern.ch

Content from this work may be used under the terms of the CC-BY-4.0 licence (© 2023). Any distribution of this work must maintain attribution to the author(s), title of the work, publisher, and DOI

ISBN: 978-3-95450-224-0 ISSN: 2673-7035 doi:10.18429/JACoW-FLS2023-TH4A2

Content from this work may be used under the terms of the CC-BY-4.0 licence (© 2023). Any distribution of this work must maintain attribution to the author(s), title of the work, publisher, and DOI

Table 1: Main Parameters of the Proposed Facility

Electron Beam	**Value**	**Unit**
Energy	240	MeV
Single-bunch charge, Q	100	pC
Nb of bunches per train	1000	
Repetition rate, f	100	Hz
Bunch length, σ_t	< 300	$\mu m/c$
Bunch spacing	1/3	ns
Normalized transverse emittance, $\epsilon^N_{x,y}$	< 3	mm mrad
Colliding Laser		
Wavelength	515	nm
Pulse energy	10	µJ
Crossing angle	2	°
Outcoming Photons		
Compton edge	2.1	MeV
Total flux, $\mathcal{F}$	2.2×10^{13}	ph/s
Bandwidth (0.5 mrad)	2.0	%
Flux (0.5 mrad)	1.6×10^{12}	ph/s
Average Brilliance, $\mathcal{B}$	4.4×10^{13}	(1)
Peak Brilliance, $\hat{\mathcal{B}}$	3.9×10^{23}	(1)

(1) ph/(s mm^2 mrad^2 0.1%BW)

Table 2: Main Parameters of the HPCI Photoinjector

Parameter	**Value**	**Unit**
Gun gradient	90	MV/m
RF pulse length	1.5	µs
Electron energy	6.5	MeV
Norm. transv. emittance	< 4	mm.mrad
Bunch energy spread	0.5	%
Bunch length	1	ps
Total length	1.3	m

modules, each comprising four 0.5 m long structures and powered by an RF unit consisting of one single klystron and a pulse compressor. The RF pulse delivered by each unit allows the acceleration of trains up to 1000 bunches per train, with a bunch spacing of 1/3 ns. The three modules are distributed with spacing 70 cm, each space including a quadrupole doublet, one beam position monitor, and two trajectory correctors.

Building on the experience made in the context of CLIC, the single-bunch charge and the iris aperture of the X-band structures were carefully tuned to optimise the RF efficiency while controlling and limiting the impact of both short- and long-range wakefields using quadrupole focusing, BNS damping, and strong damping of the high-order-modes (HOM), like envisioned for the CLIC main linac accelerating structures [1, 12, 13]. Table 3 summarises the main parameters of the linac.

Table 3: Main Parameters of the HPCI Linac

Parameter	**Value**	**Unit**
Number of modules	3	
Nb of structures per module	4	
Average gradient	35	MV/m
Structure length	0.5	m
Energy gain per module	≈ 80	MeV
Final norm. transv. emittance	< 3	mm.mrad
Final bunch energy spread	0.3	%
Total length	8.3	m

Beam Delivery

A short beam delivery section (BDS), de-magnifying and preparing the beam for the collision, was designed using three quadrupole magnets within a total length of 2.7 m starting from the linac end. Upstream the interaction point (IP), a space $L^\star = 0.6$ m was considered to accommodate the interaction chamber (IC) and some diagnostics. A dipole downstream of the IC, necessary to dump the electrons after the collision, could be used for energy measurement.

The optics of the beam delivery system was determined through a numerical optimisation of the quadrupoles' position and strength, aiming at maximising the simulated flux using a realistic 6D phase space from the linac and a realistic simulation of the ICS process obtained with RF-Track [14]. Compared with a simplistic optimisation solely based on minimising the RMS beam size at the IP, our method brought a factor 2.5 increase in the outcoming photon flux. Table 4 summarises the main parameters of the BDS.

Table 4: Main Parameters of the HPCI Beam Delivery

Parameter	**Value**	**Unit**
Number of quadrupoles	3	
Distance to IP, $L^\star$	0.6	m
Beam size at IP, $\sigma^\star_x, \sigma^\star_y$	23, 47	µm
Total length	2.7	m

Fabry-Pérot in Burst Mode

A four-mirror Fabry-Pérot cavity was considered with a bow-tie geometry. An optimisation of the burst mode parameters and the geometry was performed following the procedure presented in [15], where a detailed description of the FPC parameters is given. Burst mode parameters were obtained by maximising the effective energy in the structure, $\mathcal{E}_{\text{tot}} = \epsilon_{\text{eff}} U$, where ϵ_{eff} is the cavity effective gain, and U is the laser macropulse energy. The cavity roundtrip length of 1 m was set to a sub-harmonic of the laser repetition rate, which matches the electron bunch spacing in the linac. The FPC optimisation showed that an effective energy of 6 J could be achieved using GHz-repetition-rate high-power lasers, such as kW-Flexiburst [16].

ISBN: 978-3-95450-224-0 ISSN: 2673-7035 doi:10.18429/JACoW-FLS2023-TH4A2

Table 5: Main Parameters of the HPCI Fabry-Pérot Cavity

Parameter	Value	Unit
Round-trip length	1	m
$2d_1, 2d_2, h, R$	21.43, 28.54, 1.16, 21.46	cm
N_p, N_0, F	2292, 1298, 1000	
w_{0s}/w_{0t}	8.6/13.4	µm
Effective gain	264	
Effective energy	6	J

Start-to-End Simulation

Beam evolution simulations from the cathode to the interaction point were performed using RF-track [14], a CERN-developed tracking code that can simulate beam transport under the simultaneous effect of space-charge forces, beam loading, and short- and long-range wakefields. The simulation was performed using 1D field maps of the gun, the solenoid, and the linac structures.

The evolution of kinetic energy, normalised transverse emittance, and beam size along the HPCI injector are shown in Fig. 1. As visible, an energy of approximately 240 MeV could be attained in less than 10 m from the cathode.

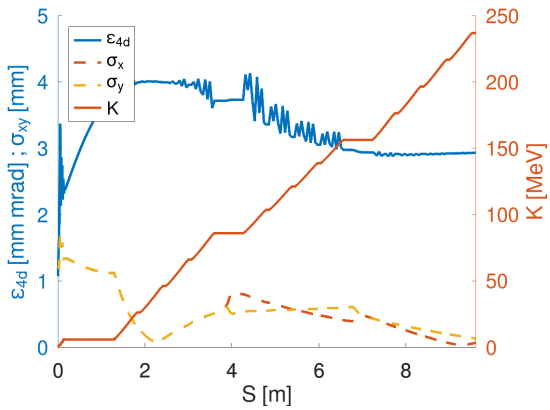

Figure 1: Evolution of the kinetic energy, the normalised transverse emittance, and the beam size along the HPCI facility, from the cathode to the linac end. The total length is 9.6 m.

The decrease of the transverse normalised emittance along the linac is related to an increase in the longitudinal emittance (not shown) due to the coupling between transverse and longitudinal planes in the accelerating structures. Despite the increase in longitudinal emittance, the projected energy spread of the bunch remained below 1%, limiting the chromatic effects in the beam delivery system and still producing ICS photons with a bandwidth under 5%.

Factors such as the amplification of single-bunch jitter due to short-range wakefields and multi-bunch jitter due to HOM in the structures were computed, indicating that the beam is largely unaffected. A value of 1.0034 was obtained for the current set-up.

ICS PHOTON PERFORMANCE

Start-to-end simulations of the setup, including photon generation, were enabled by the recent integration into RF-Track of a module simulating the ICS process directly [17]. A benchmark against the established ICS code CAIN [18] was presented in [19]. The photon performance of the HPCI-ICS source is summarised in Table 1.

The flux of the scattered photons was maximised by optimising both the electron and laser beamline. The electron gun and linac parameters from Table 2 and Table 3 were tuned to provide a 240 MeV beam with low emittance and low energy spread. The final focusing consisting of a quadrupole triplet was optimised to provide the maximum number of scattered photons per bunch. By maximising the effective energy provided by an FPC with a finesse of 1000, and tuning the FPC's geometry to allow for a high macropulse energy, a total flux of 2.2×10^{13} ph/s was obtained. The low electron beam emittance allowed for an equivalently large brilliance.

Since the ICS photon energy depends on the emission angle, the scattered photon beam is typically collimated under a collection angle to achieve a small bandwidth. For a 240 MeV electron beam, the photon beam has a natural emission angle of around 2 mrad. To achieve a photon bandwidth of 2%, the emission angle was reduced to 0.5 mrad, as shown in Fig. 2.

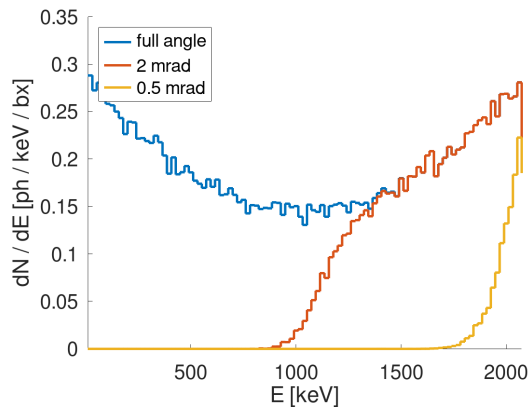

Figure 2: Scattered photon spectra from RF-Track, generated by the HPCI-ICS source. The 0.5 mrad spectrum corresponds to an energy bandwidth of 2%.

CONCLUSIONS

This paper presents HPCI-ICS, an advanced conceptual design of a compact ICS source based on an S-band photoinjector, an X-band linac, a short final focus, and a Fabry-Pérot cavity operating in burst mode, complemented by realistic beam dynamics and Compton scattering simulations. This ICS source has the potential to produce 2 MeV gamma rays with a flux of 2.2×10^{13} ph/s in less than 15 m, setting it among the most compact, high energy, and high flux source in the landscape of existing and designed ICS sources.

Content from this work may be used under the terms of the CC-BY-4.0 licence (© 2023). Any distribution of this work must maintain attribution to the author(s), title of the work, publisher, and DOI

ISBN: 978-3-95450-224-0 ISSN: 2673-7035 doi:10.18429/JACoW-FLS2023-TH4A2

REFERENCES

[1] CERN, *CERN Yellow Reports: Monographs, Vol 2 (2018): The Compact Linear e+e- Collider (CLIC) : 2018 Summary Report*, 2018. doi:10.23731/CYRM-2018-002

[2] H. Kogelnik and T. Li, "Laser Beams and Resonators", *Applied Optics*, vol. 5, no. 10, 1966. doi:10.1364/ao.5.001550

[3] A. Latina *et al.*, "A Compact Inverse Compton Scattering Source Based on X-Band Technology and Cavity-Enhanced High-Average-Power Ultrafast Lasers", in *Proc. LINAC'22*, Liverpool, UK, Aug.-Sep. 2022, pp. 31–34. doi:10.18429/JACoW-LINAC2022-MOPOJO09

[4] K. Sakaue *et al.*, "Observation of pulsed x-ray trains produced by laser-electron Compton scatterings", *Review of Scientific Instruments*, vol. 80, no. 12, 2009. doi:10.1063/1.3272789

[5] R. W. Schoenlein *et al.*, "Femtosecond x-ray pulses at 0.4 Å generated by 90° Thomson scattering: A tool for probing the structural dynamics of materials", *Science*, vol. 274, no. 5285, 1996. doi:10.1126/science.274.5285.236

[6] M. Jacquet, "Potential of compact Compton sources in the medical field", *Physica Medica*, vol. 32, no. 12, pp. 1790–1794, 2016. doi:10.1016/j.ejmp.2016.11.003

[7] D. Habs, T. Tajima, J. Schreiber, C. P. Barty, M. Fujiwara, and P. G. Thirolf, "Vision of nuclear physics with photo-nuclear reactions by laser-driven γ beams", *European Physical Journal D*, vol. 55, no. 2, 2009. doi:10.1140/epjd/e2009-00101-2

[8] J. Pruet, D. P. McNabb, C. A. Hagmann, F. V. Hartemann, and C. P. Barty, "Detecting clandestine material with nuclear resonance fluorescence", *Journal of Applied Physics*, vol. 99, no. 12, 2006. doi:10.1063/1.2202005

[9] H. Lan *et al.*, "Nuclear resonance fluorescence drug inspection", *Scientific Reports*, vol. 11, no. 1, 2021. doi:10.1038/s41598-020-80079-6

[10] A. Kostenko *et al.*, "Three-dimensional morphology of cementite in steel studied by X-ray phase-contrast tomography", *Scripta Materialia*, vol. 67, no. 3, 2012. doi:10.1016/j.scriptamat.2012.04.034

[11] R. Corsini *et al.*, "First experiments at the CLEAR user facility", in *Proc. IPAC'18)*, Vancouver, BC, Canada, Apr.-May 2018, 2018, pp. 4066–4059. doi:10.18429/JACoW-IPAC2018-THPMF014

[12] H. Zha *et al.*, "Beam-based measurements of long-range transverse wakefields in the compact linear collider main-linac accelerating structure", *Phys. Rev. Accel. Beams*, vol. 19, p. 011 001, 1 2016. doi:10.1103/PhysRevAccelBeams.19.011001

[13] A. Novohatsky, V. Smirnovn, and V. Balakin, "VLEPP: Transverse beam dynamics", in *Proceedings of the 12th International Conference on High Energy Accelerators. Batavia; Illinois*, 1983, pp. 119–120.

[14] A. Latina, "RF-Track Reference Manual", CERN, Tech. Rep., 2020. doi:10.5281/zenodo.3887085

[15] V. Musat, A. Latina, E. Granados, E. Cormier, and G. Santarelli, "An Efficient Optimisation of a Burst Mode-Operated Fabry-Perot Cavity for Inverse Compton Scattering Sources", presented at the 67th ICFA Advanced Beam Dynamics Workshop on Future Light Sources (FLS'23), Lucerne, Switzerland, Aug.-Sep. 2023, paper TU1C1, this conference.

[16] H. Ye, L. Pontagnier, C. Dixneuf, G. Santarelli, and E. Cormier, "Multi-GHz repetition rate, femtosecond deep ultraviolet source in burst mode derived from an electro-optic comb", *Optics Express*, vol. 28, no. 25, 2020. doi:10.1364/oe.409782

[17] A. Latina and V. Musat, "An Inverse-Compton Scattering Simulation Module for RF-Track", presented at the 67th ICFA Advanced Beam Dynamics Workshop on Future Light Sources (FLS'23), Lucerne, Switzerland, Aug.-Sep. 2023, paper TU4P33, this conference.

[18] P. Chen, G. Horton-Smith, T. Ohgaki, A. W. Weidemann, and K. Yokoya, "CAIN: Conglomérat d'ABEL et d'Interactions Non-linéaires", *Nuclear Instruments and Methods in Physics Research, Sect. A*, vol. 355, no. 1, 1995. doi:10.1016/0168-9002(94)01186-9

[19] V. Mușat, A. Latina, and G. D'Auria, "A High-Energy and High-Intensity Inverse Compton Scattering Source Based on CompactLight Technology", *Photonics*, vol. 9, no. 5, p. 308, 2022. doi:10.3390/photonics9050308

Content from this work may be used under the terms of the CC-BY-4.0 licence (© 2023). Any distribution of this work must maintain attribution to the author(s), title of the work, publisher, and DOI